Chapter

Relaxor Ferroelectric Oxides: Concept to Applications

Lagen Kumar Pradhan and Manoranjan Kar

Abstract

Ferroelectric ceramic is one of the most important functional materials, which has great importance in modern technologies. A ferroelectric ceramic simultaneously exhibits dielectric, piezoelectric, ferroelectric, and pyroelectric properties. The inherent ferroelectric properties are directly related to long-range electric dipoles arrangement in the ferroelectric domains and its response to external stimuli. However, the interruption of the long-range ordering of dipoles leads to the formation of a special class of material is known as relaxor ferroelectric. It shows quite different physical properties as compared to ferroelectric (normal ferroelectric). The origin and design of relaxor ferroelectric are quite interesting for fundamental perspective along with device applications. Therefore, the origin of relaxor ferroelectric along with its fundamental understanding for possible future applications, have been explained briefly in the present chapter.

Keywords: relaxor ferroelectric, spontaneous polarization, ferroelectric domains, polar nanoregions, diffuses phase transition, solid solution

1. Introduction

The origin of ferroelectricity is linked with Rochelle salt and discovered by Joseph Valasek (1897–1993) during the measurement of polarization in Rochelle salt by the applied electric field in 1920 [1]. The fundamental origin of ferroelectricity lies in the response of order parameter (electric dipole) with respect to the applied electric field. However, the field of ferroelectricity remained silent till 1940 [1]. One of the major turning points in ferroelectricity came into the picture around 1940 after the discovery of unusual behavior in dielectric properties of mixed oxides, which are crystallized to perovskite structure [1]. After that, ferroelectricity was intensively focused by the scientific community in all over the world. The perovskite compounds exhibit the ABX_3 structure, where A and B are the cations having different charges and ionic radii. "X" refers to an anion that bonded with both cations. In general, X is often Oxygen (O^{2-}) but also other ions such as sulfides, nitrides, and halides can be considered [2]. However, the perovskite compounds with the general formula ABO_3 create a distinguish place in ferroelectricity compared to others [2]. Currently different groups of perovskite compounds available in the market such as A_2BO_4-layered perovskites (ex: Sr_2RuO_4, K_2NiF_4), $A_2BB'O_6$-double perovskites (ex: Ba_2TiRuO_6) and $A_2A'B_2B'O_9$-triple perovskite (ex: $La_2SrCo_2FeO_9$), etc. [2]. Hence, ferroelectrics are fascinating groups of materials, which have extensively attracted the fundamental understanding of its complex physical properties and emerging device applications (i.e., sensors, actuators, ferroelectric random access memories,

etc.) [3]. The presence of spontaneous polarization (P) in ferroelectric material exhibits unique behavior in the presence of external stimuli such as electric field (E), temperature (T), and stress (σ). Nowadays, large numbers of reports are available on the ferroelectric properties of various kinds of materials and their possible applications in modern technologies [3]. Out of the several compounds, Lead Zirconate Titanate ($PbZr_{0.48}Ti_{0.52}O_3$/PZT) is one of the most well-known ferroelectric materials with superior ferroelectric, dielectric, and piezoelectric properties [4]. For a layman's understanding, ferroelectric materials are those which exhibit a high dielectric constant. Furthermore, normal ferroelectrics are characterized by the temperature-dependent maximum dielectric constant near ferroelectric to paraelectric phase transition temperature (T_c) and, also known as Curie's temperature [4]. Some of the basic characteristics of normal ferroelectric are the non-dispersive nature of transition temperature and follow the first-order phase transition. The temperature-dependent dielectric constant of a typical regular ferroelectric ceramic is shown in **Figure 1** [5]. Also, it is well known that the fundamental physics behind the normal ferroelectric lies in the presence of long-range order parameters (electric dipoles) in ferroelectric domains [6].

As per the literature, PZT exhibits the normal ferroelectric in nature with the above-mentioned properties and, well understood experimentally as well as theoretically. However, the spatial substitution of a foreign element such as lanthanum (La^{3+}) in PZT shows the intriguing behavior in terms of dielectric, ferroelectric and piezoelectric properties with respect to frequency, temperature, and electric field, which are different from the normal ferroelectric [7, 8]. The extraordinary properties of modified PZT are related to a special group of ferroelectric materials, which is known as relaxor ferroelectric after the name by the scientist Cross in 1987 [9]. He proposed few characteristic properties for the material to be relaxor ferroelectric, as discussed in the later section. Currently, large numbers of materials with relaxor ferroelectric behavior are available in various forms of crystal structures such as perovskite, layer perovskite, tungsten bronze structure, etc. However, the exact origin of extraordinary properties of relaxor ferroelectrics is still a matter of investigation. A series of explanations have been reported to explain the origin of relaxor behavior by using various models such as

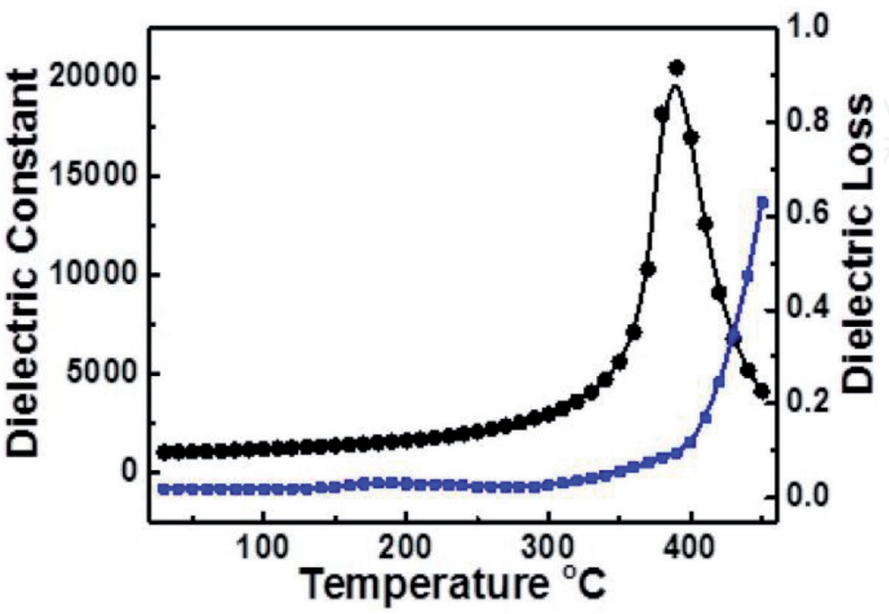

Figure 1.
Temperature-dependent dielectric constant and loss of a typical normal ferroelectric ceramic (PZT ceramic). It is adapted from Ref. [5] (open access).

diffuse phase transition model, dipolar glass model, random field model, super paraelectric model, and so on [10]. In contrast to normal ferroelectrics, the origin of relaxor ferroelectric has been correlated with the presence of compositional fluctuation induced polar nanoregions (PNRs) and tried to explain its properties up to a certain extend [10].

Due to its interesting physical properties, relaxor ferroelectrics can have possible applications in portable electronics, medical devices, pulse power devices, electric vehicles, advanced storage materials, and so on. Therefore, the different aspects from its origin to possible technological applications for future advancement have been discussed briefly in the present chapter.

2. Relaxor ferroelectrics

From the earlier discussion (introduction section), the relaxor ferroelectrics show the abnormal behavior as compared to normal ferroelectric in terms of dielectric, piezoelectric, ferroelectric properties and, subsequently, received much attention by the scientific community. To distinguish a relaxor ferroelectric, Cross assigned few basic properties as follows [9].

1. The temperature-dependent dielectric permittivity (ε') exhibits a broad and smeared maximum, which is known as a diffuse phase transition.

2. The depolarization (T_d) is defined as temperature corresponds to the steepest reduction of remanent polarization.

3. The temperatures (T_m) correspond to maximum dielectric permittivity exhibit strong frequency dependence.

4. There is no macroscopic symmetry breaking (structural changes) near-maximum dielectric temperature (T_m).

5. The Curie–Weiss (C-W) law does not follow the temperature-dependent dielectric permittivity near T_m (dielectric maxima temperature). However, Curie–Weiss law is well fitted above the T_C for normal ferroelectric. Here, T_c is the Curie temperature for normal ferroelectric.

6. Exhibits slim/constricted ferroelectric hysteresis loop due to the presence of nanosize and randomly oriented polar islands known as polar nanoregions (PNRs).

7. Existence of polar nano regions at well above the dielectric maxima temperature 'T_m' up to Burn temperature (T_B), whereas absences in the normal ferroelectrics at above the Curie temperature (T_c).

The temperature-dependent dielectric permittivity of a typical relaxor ferroelectric has been shown in **Figure 2** to visualize the different characteristic temperatures. As per the earlier reports, the interesting properties of relaxor ferroelectric are basically due to the presence of unique polar structure in nanometer size (polar nanoregions: PNRs) along with their response towards the external stimuli [11]. Therefore, it is necessary to understand the origin of PNRs and their effects on the physical properties, as discussed below.

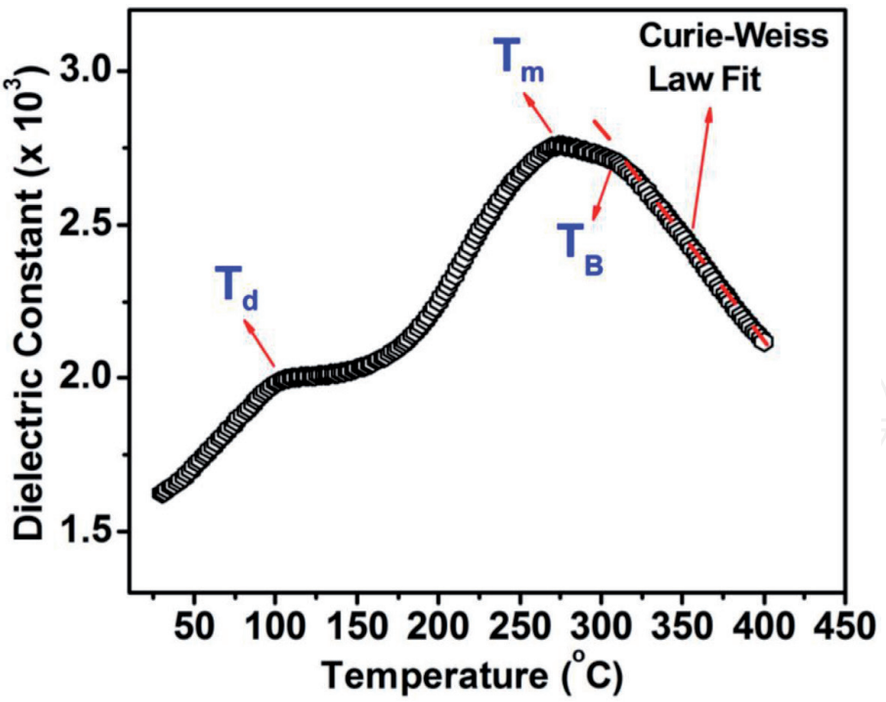

Figure 2.
Various characteristic temperatures are associated with a temperature-dependent dielectric constant of relaxor ferroelectric. Adapted from Ref. [11] and reproduced with permission (self-citation © 2021 IOP).

2.1 Polar nanoregions (PNRs)

The concept of polar nanoregions in relaxor ferroelectric is quite impressive in terms of fundamental understanding of various peculiar physical properties. Also, it has been reported that the types as well as size of the ferroelectric domains greatly influence the external factors (i.e., electric field, temperature, stress, etc.) and, consequently, affect the different physical properties [12]. Initially, several models have been proposed to describe dielectric anomalies in relaxor ferroelectrics, which lead to formulate the concept of the origin of dynamic and formation of polar nanoregions (PNRs) [10]. The conclusions of various models have been described here to correlate the abnormal behavior of relaxor ferroelectric through the presence of nanosize polar domains. Smolenskii proposed the presence of compositional fluctuation in nanometer-scale within the crystal structure by considering a statistical distribution for the phase transition temperature [13].

Furthermore, Cross extended the Smolenskii theory to superparaelectric model, which is associated with the relaxor ferroelectric behavior with thermally activated superparaelectric clusters [9]. Viehland *et al*. have reported the presence of cooperative interaction between superparaelectric clusters and forms the glass-like freezing behavior similar to the spin-glass system [14]. In later study, Qian and Bursil reported the role of random electric field on the formation and dynamic of polar clusters originated from the nanoscale chemical inhomogeneity and defects [15]. According to their theory, the dispersive nature of relaxor ferroelectric is associated with the variation of cluster size and correlation length (the distance above which the polar clusters become non-interactive) as a function of temperature. Although various models and theories have been explained the relaxor ferroelectric behavior, more additional theories and experiments need for its detailed description. Therefore, the dynamic of polar nanoregions (PNRs) with respect to an electric field as well as the temperature has been mentioned here to understand the clear picture (indirectly) of PNRs within relaxor ferroelectric in terms of dielectric and ferroelectric properties.

In the normal unpoled ferroelectric, the large-size domains with specific dipole moments are randomly distributed throughout the material. However, the domains are switched and aligned in the field direction as far as possible with the application of the threshold electric field (coercive field). This process leads to the formation of macroscopic polarization. The polarization is further enhanced with the electric field and reached to the maximum polarization (P_{max}). Usually, the normal ferroelectric exhibits large values of characteristic parameters (P_{sat}, P_r, E_c, *and* hysteresis loss) [16]. However, it is interestingly observed that the ions (cations) in parent compounds replaced by the small number of foreign ions (in terms of different ionic charge and radius) lead to break the long range ferroelectric polar order domains and, converted into a large number of polar islands which are known as polar nanoregions (PNRs) [17, 18]. In the present context, the fundamental factor related to the formation of polar nanoregions has been related to the appearance of intrinsic inhomogeneity in the material due to the compositional fluctuation at the crystallographic sites and structural modification of the unit cell. N. Qu *et al*. reported the evolution of ferroelectric domains with PNRs in the ferroelectric ceramic (refer **Figure 1** [19]). It is clearly observed that the ferroelectric hysteresis loop becomes slim (having low hysteresis loss) in nature with the increase of the percentage of nanodomains. It occurs due to the reduction of correlation length between order parameters (dipole moments). As compared to the normal ferroelectrics, it is difficult to realize the P_{max} at the moderated electric field. It is mainly due to the absence of inducing the long-range polar ordering as well as an increase in the local random field.

Furthermore, the temperature-dependent dielectric constant ($\varepsilon' \sim T$) of relaxor ferroelectric provides detailed information about the dynamic and formation of polar nanoregions (PNRs). The temperature evolution of PNRs in $(Bi_{0.5}Na_{0.5}TiO_3)$-$SrTiO_3$-$BaTiO_3$ based relaxor ferroelectric has been explained along with supported by the impedance ($Z''/Z''_{max} \sim f$) as well as electric modulus ($M''/M''_{max} \sim f$) analysis (refer Figure 11 [20]). In general, the relaxor ferroelectric exhibits the paraelectric phase at high temperature with zero net dipole moment (randomly oriented dipole moments) and well follows the Curie–Weiss law. However, the nucleation of polar nanoregions (PNRs) initiates during the cooling at the particular temperature known as Burn's temperature (T_B). This is the temperature limit below which Curie–Weiss law deviates from $\varepsilon' \sim T$ curve as shown in **Figure 4** with T_B = 286 °C [20]. Also, T_B represents the manifestation of phase transition from paraelectric to ergodic relaxor with the formation of PNRs. This observation is well supported by the occurrence of normalized impedance and electric modulus around the same frequency above the Burn's temperature. This happens due to the higher flipping frequency of the local dipoles at the high-temperature region. Further reduction of temperature ($< T_B$) leads to enhance formation of polar nanoregions (PNRs) and, subsequently, maximized in volume near dielectric maxima temperature (T_M) with broad dispersive peak, which is supported by the observation of separated normalized impedance and electric modulus peaks. The separation in peak position between Z''/Z''_{max} Vs M''/M''_{max} indirectly confirmed the maximum number of PNRs with the distribution of localized dipolar relaxation. At this temperature ($T_m \sim 150$ °C), the polar nanoregions associate with maximum number relaxation times as indicated by the broad dielectric maxima. Also, the dipole moments of PNRs are randomly distributed with approximately zero remanent polarization. The small polarized entities extend throughout the grains with different correlation lengths. Its dynamic behavior with respect to external stimuli has been observed successfully through various experiments such as in situ transmission electron microscope, neutron diffusion scattering, and piezoelectric force microscopy, and so on [21, 22]. Furthermore, the interaction between the polar nanoregions increases continuously with the reduction of temperature ($< T_m \sim 150$ °C), which leads to

initiate the freezing process of PNRs with the phase transition from ergodic to nonergodic state (ferroelectric). After that, the re-oriental flipping of polar nanoregions get a freeze at a particular temperature, known as freezing temperature (T_f) and, represented by the nonergodic state (as shown in **Figure 4** with $T_f \sim 76$ °C).

2.2 Theory of relaxor ferroelectric

As per the literature, the formation of PNRs is related to compositional fluctuation at the lattice sites of the crystal structure. To understand the fundamentals behind the formation of PNRs in the relaxor ferroelectric, ABO_3 type general perovskite compound with different charge states in A & B-site (i.e. $A'_xA''_{1-x}B'_yB''_{1-y}O_3$) can be considered. The randomness of A (A', A") and B (B′, B") sites depends upon the ionic sizes, a charge of cations, and distribution of cations in the sublattice. Depending upon the randomness, the distribution of domains is classified into two categories such as LRO (long-range order) and SRO (short-range order). SRO can be represented by the continuous with order distribution of cations on the neighboring sites, and the size of the order domains are extended in the range from 20 to 800 Å in diameter, whereas LRO is extended above 1000 Å diameter [23]. Hence, the diffuse phase transition behavior is the characteristic feature of a disordered system in which the random lattice disorder-induced the dipole impurities and defects at the crystal sites. The correlation length (r_c) in a highly ordered ferroelectric compound is defined as the extended length up to which dipole entities are correlated with each other. It is basically larger than the lattice constant (a) in normal ferroelectric and strongly dependent upon the temperature. With reducing the temperature, the correlation length increases gradually and promotes the growth of polar order in a corporative manner with long-range order in FE (ferroelectric) at $T < T_c$ [23]. However, the correlation length (r_c) in relaxor ferroelectric significantly reduced, which forms the polar nanoregions by frustrating the long-range ordering in FE similar to the dipolar glass-like behavior.

According to Landau-Devonshire theory of free energy (F) of a uniaxial ferroelectric material can be expressed in terms of electric field and polarization by ignoring the stress field as follow; [24]

$$F = \frac{1}{2}aP^2 + \frac{1}{4}bP^4 + \frac{1}{6}cP^6 + \ldots - EP \tag{1}$$

Where E is the electric field, P is electrical polarization, a, b, and c are the unknown coefficient with temperature-dependent. Here, the even powers of P are considered because the energy should be the same for $\pm P_s$. P_s is the saturation polarization. The equilibrium configuration can be estimated by finding the minima value of F [24]. The phenomenological description of ferroelectrics states that the spontaneous polarization varies continuously with temperature and attains zero value at the Curie's temperature (T_c: dielectric maxima temperature) in normal ferroelectric. However, the properties of relaxor ferroelectrics, which depend upon polarization in the order of P^2 have been measured experimentally at above the maximum dielectric temperature (shown in **Figure 3**), which supported the presence of polar nanoregions (PNRs) [25, 26]. Furthermore, different formulations have been extensively used to estimate the various characteristic parameters and the degree of relaxor ferroelectric behavior (diffuseness) of materials as described below.

The relaxor ferroelectrics exhibit the broad diffuse maxima in the temperature dependence dielectric permittivity. For a typical RFE, strong dispersion behavior of

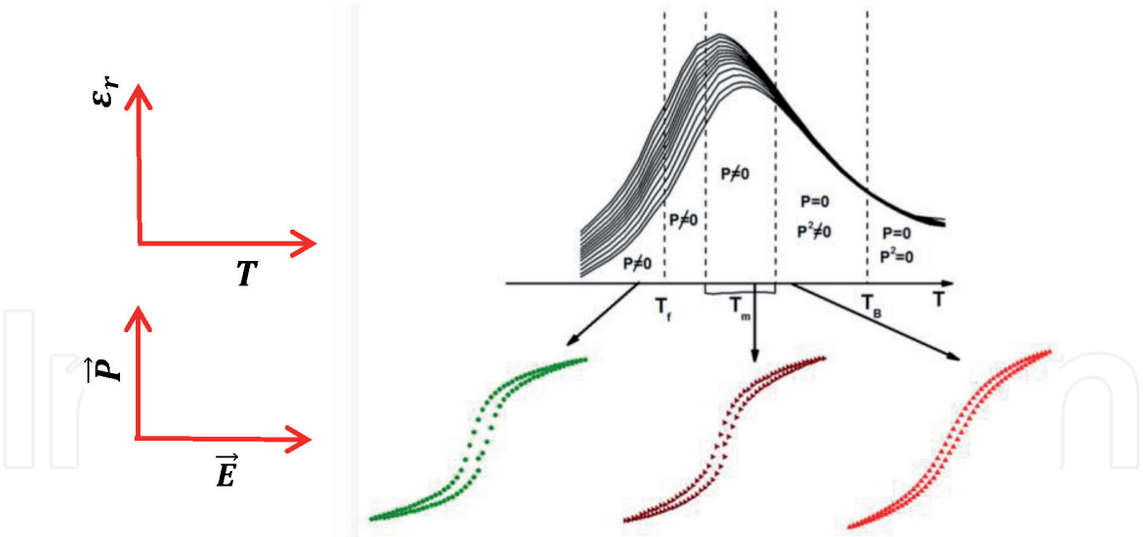

Figure 3.
Confirmation of the presence of polar nanoregions at above the maximum dielectric temperature (T_m), ε_r', T, $\vec{P}$ and E are the permittivity, temperature, electrical polarization, and electric field, respectively. Adapted from ref. [23] (open access).

dielectric permittivity $\varepsilon'(T,\omega)$ with applied frequency observes at the lower side of dielectric maxima temperature (T_m) and becomes independent at the higher temperature region. Also, the T_m shifts towards the higher temperature with an increase in frequency, which is clearly shown in **Figure 3**. Also, the reduction in relaxation processes below T_m in RFEs suggests the onset of relaxor freezing. Therefore, the characteristic relaxation time diverges near freezing temperature (T_f) as per the following Volgel-Fulcher (VF) law relation [27, 28].

$$f = f_0 \exp\left(\frac{-E_a}{K_B\left(T_m - T_f\right)}\right) \tag{2}$$

Here, f is the measuring frequency, and E_a, T_f an f_0 are the parameters. In general, T_f is believed to be the temperature corresponds to freezing of the dynamic of PNRs due to the increase in the cooperative interaction between them. A typical VF relation for $BiAlO_3$-(x) $BaTiO_3$ solid solution with x = 0.05 and 0.1 has been shown in **Figure 4** [29].

Furthermore, the Curie–Weiss (C-W) law is well known to describe the ferroelectric to paraelectric phase transition for normal ferroelectric and, well fitted above the phase transition temperature (Curie temperature: T_c). However, it deviates for relaxor ferroelectrics due to the presence of diffuse phase transition. Therefore, reciprocal of *C-W* law can be used to estimate the degree of deviation (diffuseness) for RFEs by the following relation [30].

$$1/\varepsilon_r' = \frac{T - T_c}{C} \tag{3}$$

Here, ε_r' is the dielectric permittivity, C is the Curie temperature. It has been explained that, the C-W law is well fitted at above the Burn's temperature (T_B). Hence, the degree of diffuseness (ΔT) in term of temperature can be calculated as follow. [31, 32]

$$\Delta T = T_B - T_m \tag{4}$$

To visualize the above relations for the experimental observations, the fitted curve has been shown in **Figure 5** [11]. The separation between maximum dielectric temperature and Burn temperature represents the characteristic of diffuse phase transition.

Furthermore, Uchino and Nomura quantified the dielectric material's relaxor behavior from the ferroelectric to the paraelectric phase transition. They have estimated the diffuse behavior by employing the modified Curie–Weiss (MCW) law. According to this law, the reciprocal of the permittivity can be expressed as; [33].

$$\frac{1}{\epsilon'} - \frac{1}{(\epsilon_{\max})'} = C(T - T_m)^{\gamma} \; 1 \le \gamma \le 2 \tag{5}$$

Here γ and C are the constants. γ = 1 for the normal ferroelectric material. $1 \le \gamma \le 2$ represents the relaxor ferroelectric behavior and, $\gamma = 2$ is known as the completely diffuse phase. The MCW law is well fitted for $(La_x(Bi_{0.5}Na_{0.5})_{1-1.5x})_{0.97}Ba_{0.03}TiO_3$ based relaxor ferroelectric with different mole fraction of La (refer **Figure 3** [34]).

According to Smolenskii's work, the temperature dependence of dielectric permittivity above T_m is extensively studied to explain the DPT (diffuse phase transition) of relaxor ferroelectrics. Besides this, there are other models reported to describe DPT behavior quantitatively at above the maximum dielectric temperature ($T > T_m$). One of the most applied models is based on Lorentz-type empirical relation as follow [35, 36].

$$\frac{\varepsilon_A}{\varepsilon_r} = 1 + \frac{(T - T_A)^2}{2\delta_A^2} \tag{6}$$

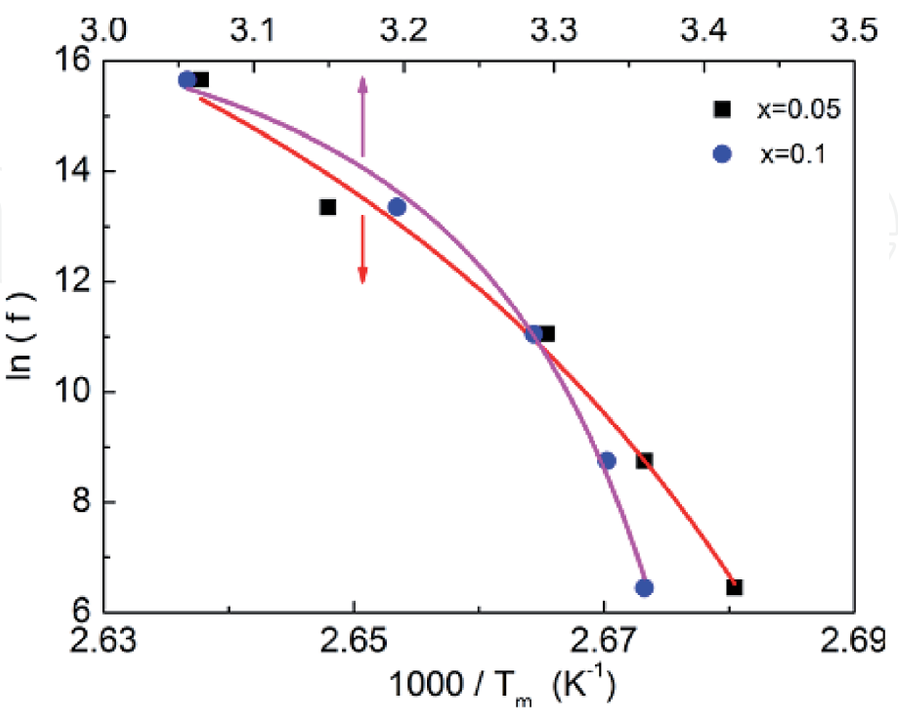

Figure 4.
Volgel-Fulcher relation plot for $BiAiO_3$-(x) $BaTiO_3$ solid solutions with x = 0.05 & 0. Adapted from ref. [29] and reproduced with permission (© 2021 AIP).

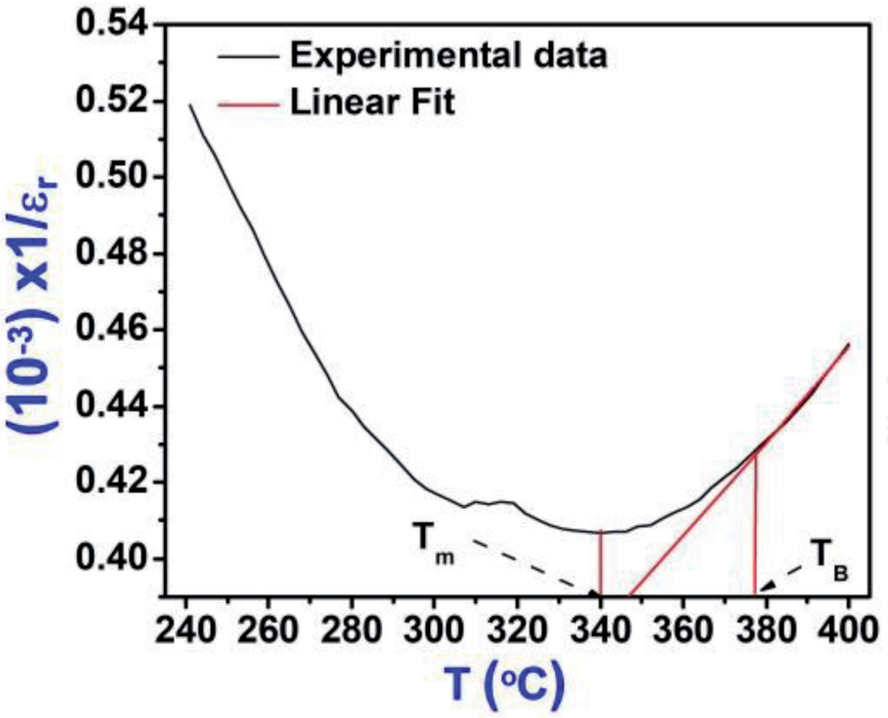

Figure 5.
Variation of $\frac{1}{\varepsilon_r}$ *as a function of temperature, and the solid straight lines represent the C-W law at a particular frequency.* T_B *is the burn temperature. Adapted from ref. [11] and reproduced with permission (self-citation © 2021 IOP).*

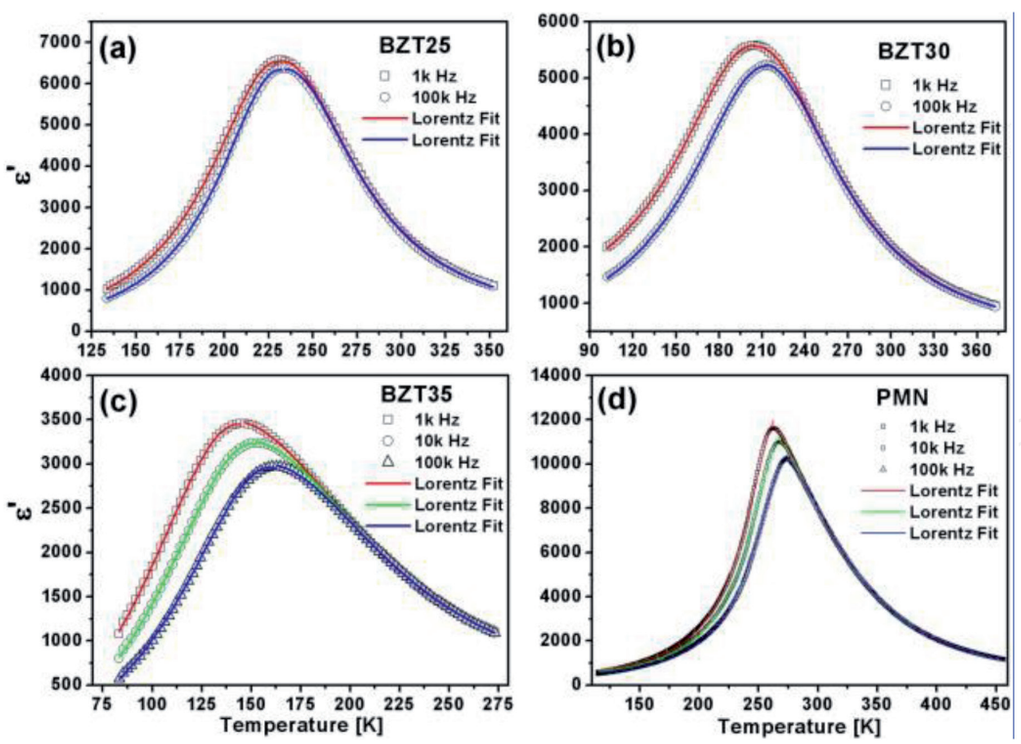

Figure 6.
The temperature-dependent dielectric permittivity of (a) BZT25 (b) BZT30, (c) BZT35 and (d) PMN ceramic fitted with Lorentz relation (solid lines). Adapted from ref. [37] and reproduced with permission (© 2021 AIP).

Where T_A ($T_A \neq T_m$) and ε_A are the fitting parameters. T_A can be defined as the temperature corresponding to the dielectric peak and ε_A is the dielectric constant at T_A. δ_A is the diffuseness parameters which is independent of temperature and

frequency. Hence, the DPT behavior of RFEs represents in terms of temperature (T_m-T_A) and dielectric constant ($\varepsilon_r - \varepsilon_A$). Lei *et al*. have reported that the Lorentz formula is well fitted in both lower and higher temperature regions in $\varepsilon_r \sim T$ curve for Ba $(Ti_{0.8}Sn_{0.2})O_3$ relaxor ferroelectric [37]. Similarly, Lorentz type relationship in temperature-dependent dielectric permittivity in Ba $(Zr_xTi_{1-x})O_3$ solid solutions, $PbMg_{1/3}Nb_{2/3}O_3$ relaxor with diffuse phase transition has been reported by S. Ke *et al*. A typical plot of Lorentz formula is shown in **Figure 6**.

3. Materials aspects

Currently, there are several classes of relaxor ferroelectrics available based on different compositions. However, the existing relaxor ferroelectrics are further modified with suitable foreign elements to tune the physical properties. On the basis of material aspect, the relaxor ferroelectrics are classified into two categories as lead-based and lead-free relaxor ferroelectrics. In the present scenario, the lead-based RFEs are dominated extensively on the commercial market due to their superior dielectric, ferroelectric and piezoelectric properties. However, the restriction of lead-based compounds due to their environmental issue (toxic in nature) leads to an increase in the demand for lead-free relaxor ferroelectrics. Therefore, lead-based and lead-free relaxor ferroelectrics are briefly discussed [38, 39]. In addition, the concept of morphotropic phase boundary has been discussed to understand the formation of various solid solutions.

3.1 Concept of morphotropic phase boundary

This term is very common in the field of complex ferroelectric solid solutions. Basically, the term 'morphotropic' referred to the crystal phase transition due to the change in the composition and which is different from the polymorphic phase boundary (PPB) [40]. PPB is generally referred to as a change in phase transition with respect to the temperature. Morphotropic phase boundary represents the phase transition between rhombohedral and tetragonal ferroelectric phases with respect to the variation of composition or pressure. In the vicinity of MPB, the materials exhibit maximum dielectric and piezoelectric properties due to the presence of structural inhomogeneity [41]. The most common and well-known ferroelectric material, i.e., Lead Zirconate Titanate [$Pb(Zr_{0.52}Ti_{0.48})TiO_3$/PZT] lies near morphotropic phase boundary (MPB), as shown in **Figure 7**. Basically, PZT solid solution is the competing of coexistence phases, i.e., $PbZrO_3$ with rhombohedral symmetry (*R3c*) and $PbTiO_3$ with tetragonal symmetry (*P4mm*) as shown in **Figure 7**. However, the origin of extraordinary physical properties near MPB is still a matter of debate. In recent years, researchers have been drawn attention towards preparing solid solutions near MPB of different ferroelectric oxides [41]. The MPB composition of PZT is associated with the 14 possible polarization axis (i.e., 6 from tetragonal and 8 from the rhombohedral), which leads to reduce the energy barrier (i.e., Landau free energy) of the crystal system and, subsequently enhanced the piezoelectric, dielectric, and ferroelectric properties. The dielectric, polarizability, and electromechanical coefficients can be further increased by modifying MPB composition with different suitable acceptors or donor dopants [41].

3.2 Lead-based relaxor ferroelectrics

The most widely used ferroelectric materials for the different applications are derived from the solid solution of (x) $PbTiO_3$-(1-x) $PbZrO_3$. The lead-based

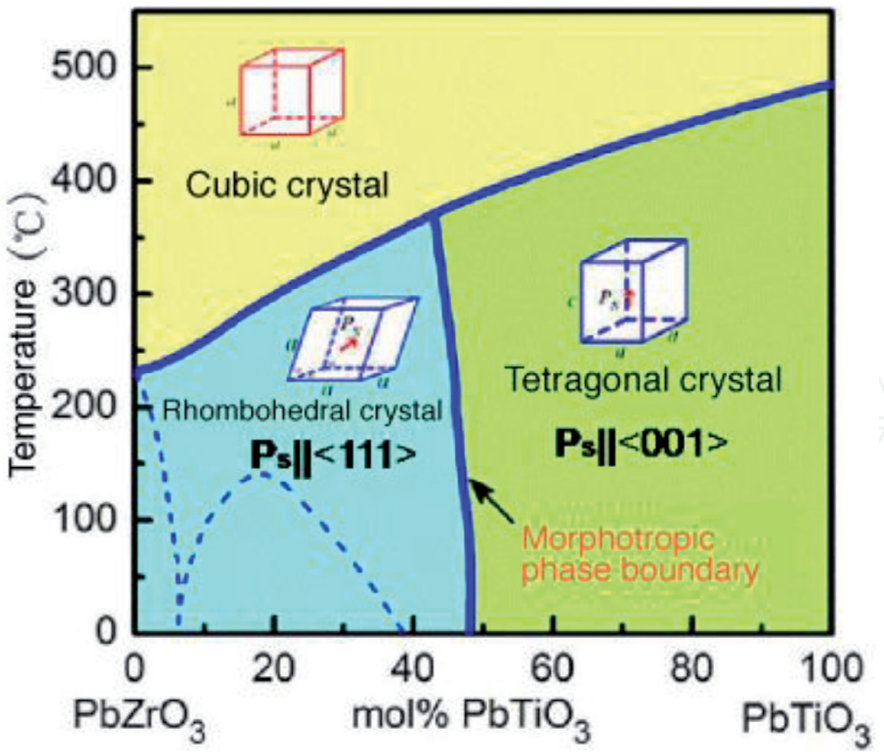

Figure 7.
Lead Zirconate Titanate (PZT) solid solution near morphotropic phase boundary (MPB) composition between $PbZrO_3$ with rhombohedral symmetry (R3c) and $PbTiO_3$ tetragonal symmetry (P4mm). Adapted from ref. [41] (open access).

solid solutions exhibit different characteristics properties ranging from normal ferroelectric-relaxor- antiferroelectric. Therefore, the lead-based relaxor ferroelectrics are quite important for the modern device industries. To date, the PZT is considered a vastly used piezoelectric material. The relaxor properties in PZT have been successfully developed by incorporating foreign elements in A/B sites with isovalent and aliovalent dopants (donor and acceptor dopants). Some of the dopants which have been used in the PZT crystal system are as follows: Isovalent types (Ba^{2+}, Sr^{2+} for Pb^{2+} site & Sn^{4+} for Zr^{4+} and Ti^{4+} sites), Donor types (La^{3+}, Nd^{3+}, Sb^{3+} for Pb^{2+} sites & Nb^{5+}, Ta^{5+}, Sb^{5+}, W^{6+} for Zr^{4+} and Ti^{4+} sites) and acceptor types (K^{+}, Na^{+} for Pb^{2+} & Fe^{3+}, Al^{3+}, Sc^{3+}, In^{3+}, Cr^{3+} for Zr^{4+} and Ti^{4+} sites). Other than PZT, the lead-based relaxor ferroelectrics are $Pb(Mg_{1/3}Nb_{2/3})O_3$(PMN) or $Pb(Sc_{1/2}Ta_{1/2})O_3$(PST), $Pb_{1-x}La_x(Zr_{1-y}Ti_y)_{1-x/4}O_3$(PLZT),$Pb(Zn_{1/3}Nb_{2/3})O_3$(PZN) $Pb(Mg_{1/3}Ta_{2/3})O_3$(PMT), $Pb(Sc_{1/2}Nb_{1/2})O_3$(PSN),$Pb(In_{1/2}Nb_{1/2})O_3$(PIN), $Pb(Fe_{1/2}Nb_{1/2})O_3$(PFN), $Pb(Fe_{2/3}W_{1/3})O_3$(PFW) and the solid solutions:$(1-x)Pb(Mg_{1/3}Nb_{2/3})O_3$-$xPbTiO_3$(PMN-PT) and $(1-x)Pb(Zn_{1/3}Nb_{2/3})O_3$-$xPbTiO_3$ (PZN-PT) [42–45]. Therefore, few recent experimental results of lead based ferroelectrics have been explained here to understand the formation and dynamic of PNRs. As per the literature, (1-x) $[Pb(Mg_{1/3}Nb_{2/3})O_3]$-(x) $[PbTiO_3]$ solid solution exhibit normal ferroelectric properties near MPB (x = 0.30 to 0.35) [46]. Also, the structural fluctuation from rhombohedral to tetragonal through intermediate phases (i.e. monoclinic/orthorhombic/triclinic) has been observed with respect to x vary from 0.13 to 0.30. The relaxor properties in above solid solution have been developed (refer **Figures** 5 and 7 [46]) with substitution of optimum mole fraction (4%) of Sr^{2+} in place of Pb^{2+}. The formation of compositional fluctuation leads to form short-range order PNRs and, subsequently, reduces the remanent polarization and coercive field and the appearance of diffuse phase transition. The presence of PNRs significantly enhanced the dispersive nature of dielectric permittivity with frequency [46].

3.3 Lead-free relaxor ferroelectrics

Although lead-based relaxor ferroelectrics are dominating in the electronic markets, lead-free ceramics have been focused intensively for last few years due to the restriction of hazardous substances such as lead, lead oxide and heavy metals. There is no equivalent alternative as compared to lead-based compounds, particularly PZT based relaxor ferroelectrics till now. However, certain lead-free relaxor ferroelectric groups with a perovskite crystal structure are impressed by the current researchers for their enhanced physical properties in terms of dielectric, ferroelectric, and piezoelectric properties. Those relaxor ferroelectrics are typical classified as follows: (a) barium titanate ($BaTiO_3$/BTO) based-, (b) potassium sodium niobate ($K_{0.5}Na_{0.5}NbO_3$/KNN) based-, (c) bismuth sodium titanate ($Bi_{0.5}Na_{0.5}TiO_3$/BNT) based- and (d) bismuth layer structured ferroelectrics (BLSFs) [47].

3.3.1 BTO based relaxor ferroelectrics

At room temperature, BTO exhibits stable electrical properties (dielectric and ferroelectric), good electrochemical coupling (k_{33} ~ 0.50), high-quality factor, low dielectric loss, but limited by low T_c (120 °C–135 °C) and d_{33} (~190 pC/N). Also, it follows the subsequent structural phase transitions from cubic (>120 °C–135 °C)-tetragonal (120 °C to 20 °C)-orthorhombic (20 °C to −80 °C)-rhombohedral (<−80 °C). In general, $BaTiO_3$ exhibits normal ferroelectric and follows the Curie–Weiss law at ferroelectric to the paraelectric phase transition. The $BaTiO_3$-$BaSnO_3$ solid solution was the first BTO based compound in which relaxor ferroelectric behavior was observed. After that, the relaxor behavior in BTO has been developed by designing the A and B-sites with incorporation of both heterovalent and isovalent ionic substitutions. Currently, there are several modified BTO ceramics available with diffuse phase transition. The available BTO based relaxor ferroelectric systems are $BaTiO_3$-$CaTiO_3$, $BaTiO_3$-$BaZrO_3$-$CaTiO_3$ [d_{33} ~ 620pC/N for $Ba_{0.85}Ca_{0.15}Ti_{0.90}Zr_{0.10}O_3$], $BaTiO_3$-$BiFeO_3$-$Bi(Mg_{0.5}Ti_{0.5})O_3$, $BaTi_{0.8}Sn_{0.2}O_3$, $Ba(Ti_{0.94}Sn_{0.03}Zr_{0.03})O_3$ $BaTiO_3$–$La(Mg_{0.5}Ti_{0.5})O_3$, $BiTiO_3$-(x) $Bi(Mg_{2/3}Nb_{1/3})O_3$ and so on [47–49].

3.3.2 KNN based ceramic system

The KNN system is one of the most promising lead-free alternatives due to its high T_c (~410 °C), high P_r (~33μcm^{-2}), and large K_p (~0.454). Basically, KNN is the solid solution of two perovskite compounds, i.e., $KNbO_3$ (orthorhombic: ferroelectric) and $NaNbO_3$ (orthorhombic: antiferroelectric). In general, the KNN forms the morphotropic phase boundary as similar to PZT [47]. It exhibits moderate dielectric, ferroelectric and piezoelectric properties as compared to PZT. Similar to BTO, the relaxor behavior of KNN has been developed by introducing other elements through interrupting the long rang polar ordering and, forms the PNRs as evidenced by several experimental results. Some of the KNN based relaxor ferroelectrics with physical properties are $(K_{0.48}Na_{0.535})_{0.942}Li_{0.058}NbO_3$ [d_{33} ~ 314, K_{33} ~ 41,T_c ~ 490 °C], $(K_{0.44}Na_{0.52}Li_{0.04})(Na_{0.86}Ta_{0.10}Sb_{0.04})O_3$ [d_{33} ~ 416pC/N],$0.96(K_{0.5}Na_{0.5})_{0.95}Li_{0.05}Nb_{1-x}Sb_xO_3$–$0.04BaZrO_3$, 0.5wt%Mn-KNN ($T_c$ ~ 416 °C, d_{33} ~ 350 pCN^{-1}), $(Na_{0.44}K_{0.515}Li_{0.045})Nb_{0.915}$ $Sb_{0.045}Ta_{0.05}O_3$(d_{33} ~ 390pC/N, T_c ~ 320 °C K_{33} ~ 0.49), $0.96(K_{0.4}Na_{0.6})(Nb_{0.96}Sb_{0.04})O_3$–$0.04Bi_{0.5}K_{0.5}Zr_{0.9}Sn_{0.1}O_3$ (d_{33} ~ 460pC/N, T_c ~ 250 °C, K_{33} ~ 0.47),$(Na_{0.5}K_{0.5})_{0.975}Li_{0.025}Nb_{0.76}$ $Sb_{0.06}Ta_{0.18}O_3$ (d_{33} ~ 352, T_c ~ 200 °C, K_{33} ~ 0.47) [48, 50].

3.3.3 BNT based ceramic systems

BNT is one of the promising lead-free materials to compete with PZT for actuator applications. It exhibits relaxor ferroelectric properties with relatively large remanent polarizations (P_r ~ 38 μC/cm^2), large coercivity (E_c ~ 73 kV/cm), and high Curie temperature (~320 °C). It follows the character of an ergodic relaxor with room temperature rhombohedral crystal symmetry. The physical properties of several BNT based binary and solid ternary solutions near MPB composition along with the substitution of various cations have been reported; such as BNT-$ATiO_3$ (A = Ca^{2+}, Sr^{2+}, $Ba^{2+,}$ and Pb^{2+}), BNT-$KNbO_3$, BNT-$Bi_{0.5}Li_{0.5}TiO_3$, BNT-$Bi_{0.5}K_{0.5}TiO_3$(BNT-BKT), BNT-$K_{0.5}Na_{0.5}NbO_3$(BNT-KNN), BNT-BKT-KNN, BNT-BT-KNN, BNT-BKT-$BiFeO_3$, BNT-BKT-$BaTiO_3$-$SrTiO_3$ and so on [50, 51].

3.3.4 Bismuth layer structured ferroelectrics (BLSFs)

Recently, BLSFs are considered as lead-free relaxor ferroelectrics due to its excellent fatigue properties. The general formula of BLSFs is $(Bi_2O_3)^{2+}$ $(A_{m-1}B_mO_{3m+1})^{2-}$ with A-site occupy by mono-, di- or trivalent ions, B-site occupies by tetra-, penta- or hexavalent ions with appropriate size [47]. The possible A-site elements could be K^+, Na^+, Ca^+, $Sr.^+$, Pb^{2+}, Ba^{2+}, La^{3+}, Bi^{3+}, Ce^{3+}, etc. and B-site could be Ti^{4+}, Nb^{5+}, Ta^{5+}, W^{6+}, Mo^{6+}, etc. The number "m" (=1, 2, 3, 4, and 5) is the number of BO_6 octahedra in the $(A_{m-1}B_mO_{3m+1})^{2-}$ perovskite blocks. BLSFs exhibit high T_c, low tanδ, low ε_r, and decent aging resistance. The above mentioned various classes of relaxor ferroelectrics exhibit different unique relaxor behavior depending upon the formation of PNRs due to the compositional fluctuation in the crystallographic sites.

4. Possible applications

The relaxor ferroelectrics can have wide range of technological applications due to its intriguing physical properties in terms of dielectric, ferroelectric and piezoelectric. As per the earlier discussion, the fundamental origin of unusual behavior in RFEs is mainly due to the presence of polar nanoregions (PNRs). In this section, few important applications of RFEs in modern technologies based on the specific physical property have been briefly discussed for the scientific community. In addition, the systematic approaches have been formulated for individual properties.

i. Currently, the electrical energy storage systems (EESSs) with high energy density and power density are the essential components for the various types of electronics. Out of several EESSs, dielectric capacitors (DCs) are widely used for delivering energy due to its high power density (PD). Power density (P) is defined as the amount of energy delivered by the device per unit time per unit volume. It can be defined as; [52]

$$P = \frac{W_e}{tV} \tag{7}$$

Where, W_e is the energy storage by the device, t and V are the time and volume, respectively. To obtain a high power density, it is essential to increase the energy storage density of the device. The energy storage density of DCs directly related to the dielectric displacement (D) and external applied electric field (E) by the following relation [52].

$$W_e = \frac{1}{2}\varepsilon_r E_b^2 \tag{8}$$

Where ε_r is the relative dielectric permittivity of the material and E_b is the electric field corresponding to the breakdown strength (BDS). However, the high electric field (high BDS) requires high energy storage in the linear dielectric materials. Hence, it creates the hindrance for portable and compact device applications. On the other hand, ferroelectric materials are the possible option to use for energy storage devices at the moderate electric field. Different characteristic parameters related to the energy storage capacity of a nonlinear dielectric material (ferroelectric) are mentioned here [53].

$$\text{Total energy storage density}: W_{store} = \int_0^{P_{\max}} E\,dP \tag{9}$$

$$\text{Total recovery energy density}\left(\text{useful energy}\right): W_e = \int_P^{P_{\max}} E\,dP \tag{10}$$

$$\text{Efficiency of useful energy storage density}: \eta\,(\%) = \frac{W_e}{W_{store}} = \frac{W_e}{W_e + W_{loss}} \times 100 \tag{11}$$

Where $P_{\max}$ and P_r are the maximum polarization and remanent polarization of the ferroelectric hysteresis loop, respectively. E is the applied electric field. W_{loss} is the total loss of energy storage density. Therefore, the ferroelectric materials' energy storage density can be enhanced by increasing the difference between maximum

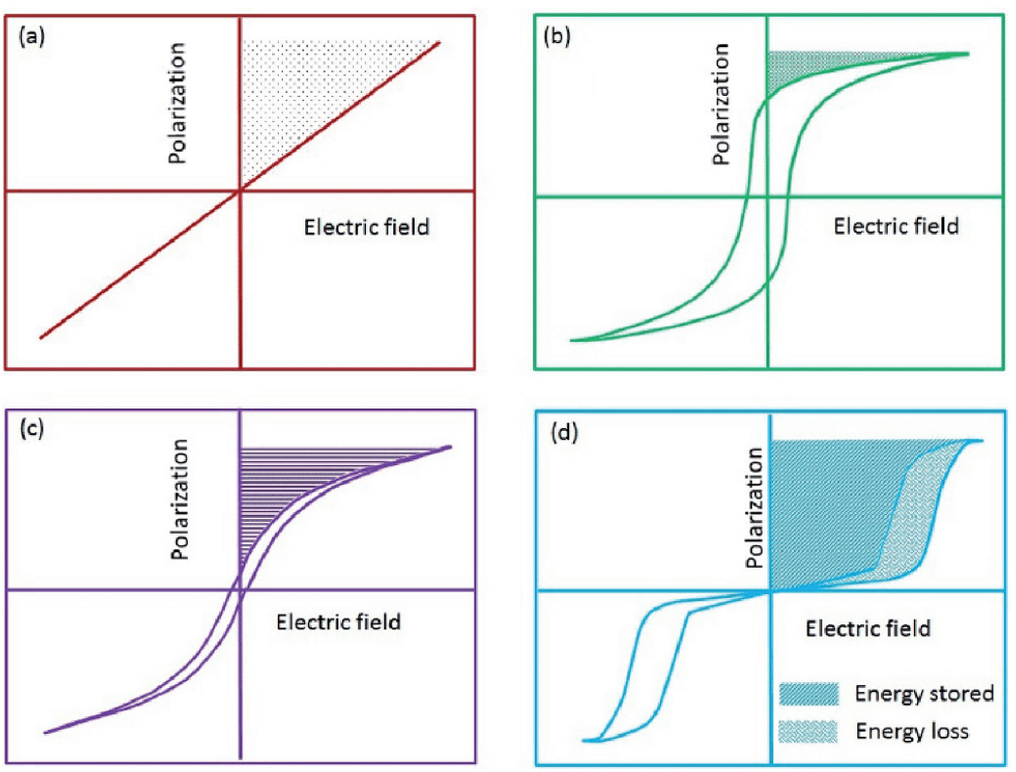

Figure 8.
Typical polarization versus electric field with energy storage capacity and energy loss of different dielectric materials (a) linear, (b) ferroelectric, (c) relaxor ferroelectric, and (d) antiferroelectric. Adapted from ref. [54] (open access).

polarization (P_{max}) and remanent polarization (P_r). A brief description of various dielectric materials' energy storage density is shown pictorially in **Figure 8** [54].

Out of the different dielectric materials, antiferroelectrics exhibit the highest energy storage density. However, there are certain limitations of antiferroelectric which hindrance for its technological applications, such as; few availability (mostly lead-based) and less life cycles (i.e., degradation of antiferroelectric behavior with time). Hence, relaxor ferroelectrics become important for the dielectric capacitor with high energy storage density along with power density due to its slim/constricted ferroelectric hysteresis loop.

ii. Nowadays, refrigerators are widely used as an essential requirement in various sectors starting from household to industrial applications. Basically, the refrigerator is the process to keep cooling a space or substance at below room temperature. The most popular refrigerator process is based on the vapor-compression of the refrigerant [55]. The most common refrigerant used for cooling purposes is chlorofluorocarbons (CFC), which is toxic in nature and cause the Ozone layer depletion. Therefore, several alternative methods have been developed for the cooling system. Out of that, electrocaloric effect based refrigerator becomes one of the emerging cooling technologies that evolved recently. The Electrocaloric (EC) effect observes in the materials having dipolar entities (electric dipoles) and depends upon the interaction between an electric field with the order parameter (dipole moments), which leads to varying the randomness (entropy) of the dipoles in the system [55]. The change in entropy of the material leads to heating or cooling of the respective system under adiabatic conditions. One can refer to the details on electrocaloric effect, including theory, measurement, and application, as reported by Z. Kutnjak *et al.* [56]. Therefore, the EC effect is directly related to the degree of disorder in the materials. As per the material prospective, relaxor ferroelectrics exhibit a higher EC effect than normal ferroelectric due to the presence of a larger number of short-range order polar islands, i.e., polar nanoregions (PNRs).

There are different ways to estimate the entropy change in the materials and subsequently quantified the electrocaloric effect for technological applications. Among them, the indirect method has been widely employed for different systems by the scientific community to calculate the entropy (ΔS) as well as temperature change (ΔT) of the material as mentioned below [56].

$$\Delta S = -\frac{1}{\rho}\int_{E_1}^{E_2}\left(\frac{\partial P}{\partial T}\right)_E dE \tag{12}$$

$$\Delta T = -\frac{1}{\rho}\int_{E_1}^{E_2}\frac{T}{C}\left(\frac{\partial P}{\partial T}\right)_E dE \tag{13}$$

Here, ρ is the density of the sample. The pyroelectric ratio $\left(\partial P/\partial T\right)_E$ can be estimated from the polarization-temperature (P–T) curve. C is the specific heat of the material, E_1 and E_2 are the initial and final applied electric fields, respectively. ΔT is the change in temperature with the applied electric field. Some of relaxor ferroelectrics in bulk as well as thin film form are $Pb_{0.92}La_{0.08}Zr_{0.65}Ti_{0.35}O_3$ thin film (ΔT = 3.5 K at 700 kV/cm), [57] $[Bi_{0.5}(Na_{0.72}K_{0.18}Li_{0.1})_{0.5}]_{1-x}Sr_xTiO_3$ (ΔT = 2.51 K at 65 kV/cm), [58] $Ba_{0.85}Ca_{0.15}Zr_{0.10}Ti_{0.90}O_3$ (ΔT = 1.479 K at 60 kV/cm), [59] $0.65(0.94Na_{0.5}Bi_{0.5}TiO_3–0.06BaTiO_3) - 0.35SrTiO_3$ thin film ($\Delta T \sim 12$ K at 2738 kV/cm) [60] and so on.

iii. Recently, the electric field-induced strain (electromechanical property) in ferroelectric ceramics has focused intensively due to their wide range of applications in sensors, actuators, MEMS, medical ultrasonic imaging, and so on. In a nutshell, the degree of induced strain in a material can be represented by the parameter S_{max}/E_{max}. Hence, there are two ways to increase the overall strain performance (d_{33}: piezoelectric strain coefficient), i.e. either increase the maximum strain (S_{max}) or reducing the driving electric field (E_{max}). It is well known that, PZT exhibits outstanding electromechanical properties due to the structural instability between rhombohedral and tetragonal crystal symmetries near morphotropic phase boundary [61]. In general, the non-ergodic relaxor phase shows the irreversibly high piezoelectric coefficient (d_{33}) with minimum electrostrain due to the inverse piezoelectric effect. However, compositional fluctuation induced non-ergodic to ergodic relaxor exhibit large repeatable strain due to the phase transition from ergodic relaxor to electric field induce intermediate/metastable ferroelectric phase. The main difference between ergodic and non-ergodic relaxor states is the presence of PNRs. The evolution of PNRs size with respect to the applied electric field plays an important role on the recoverability of the electric field-induced phase transition. Therefore, the ergodicity of relaxor ferroelectric can be enhanced by substituting heterovalent ions that alter the local random electric field and subsequently increase the overall electrostrain. B. Gao *et al.* reported the unexpectedly high piezoelectric response in Sm doped PZT54/46 with d_{33} ~ 590 pC/N, kp ~ 57.1% and S_{max} ~ 0.31% [62].

Some of the reported relaxor ferroelectrics are BNT-BKT-Bi$(Ni_{2/3}Nb_{1/3})O_3$ solid solution (S_{uni} ~ 0.51% at 65 kV/cm, d_{33} ~ 890 pm/V at 45 kV/cm),[63] 0.66PNN-0.34PT (d_{33} ~ 560 pC/N),[64] 0.97[0.94$Bi_{0.5}Na_{0.5}TiO_3$–0.06$BaTiO_3$]-0.03$AgNbO_3$ (d_{33} ~ 721 pm/V at 60 kV/cm),[65] (BNKT–BST–La0.020 (S_{max} ~ 0.39%, d_{33} ~ 650 pm/V) [66] and so on. In addition, novel semiconductor-relaxor ferroelectric based 0–3 type composite has been reported for high temperature piezoelectric applications. Those are ZnO (semiconductor)-(BNT-BTO) (relaxor ferroelectric), ZnO- (BZT-BCT), etc. [67].

iv. Due the multifunctionality of ferroelectrics, it has wide range of applications in modern technologies. Out of that, voltage control dielectric permittivity behavior of ferroelectric is widely used for microwave devices such as resonators, phase shifters, filters and so on [68]. For these applications, the material's tunability (change in capacitance with applied DC bias) should be high with a minimum loss factor. For normal ferroelectrics, tunability attends maximum value near transition temperature i.e. Curie's temperature and hence, different materials can be used for different applications [69]. For example, $SrTiO_3$ like materials are useful at cryogenic temperature, whereas $BaTiO_3$ and PZT are most suitable for room temperature. As per the fundamental aspect, the tunability of a material directly depends on how fast the dipoles respond to the external electric field. The following relations can be used to estimate the tunability quantitatively [69].

$$Tunability(\%) = \frac{\varepsilon(E_0) - \varepsilon(E)}{\varepsilon(E_0)} \times 100\% \tag{14}$$

Where, $E_0 =$ 0 kV/cm, and E is the electric field at which the tunability to be measured. In addition to high tunability, high $Q = 1/tan\delta$ or low loss requires to reduce the power loss. Overall, the figure of merit (FOM) for a dielectric tunability material is an important parameter to select the material for applications [69].

$$FOM\left(K\ factor\right) = tunability \times Q = \frac{\varepsilon\left(E_0\right) - \varepsilon\left(E\right)}{\varepsilon\left(E_0\right)} \times 1/tan\delta \tag{15}$$

Interestingly, it has been observed that the tunability in relaxor ferroelectric exhibits a higher value as compared to normal ferroelectrics. It happens due to the presence of short-range ordering PNRs, which respond very quickly with the applied electric field compared to the long-range ordering of dipoles in normal ferroelectrics. Maiti *et al.* reported the lead free relaxor ferroelectric $Ba(Zr_{0.35}Ti_{0.65})O_3$ with room temperature tunability ~44% and K-factor ~ 234 at 40 kV/cm [69]. Similarly, Z. Liu *et al* reported the tunable dielectric properties of $K_{0.5}Na_{0.5}NbO_3$-(x) $SrTiO_3$ (x = 0.16, 0.17, 0.18, 0.19) relaxor ferroelectric with highest tunability ~31.6% for x = 0.16 [70]. There are other relaxor ferroelectrics available in literature having tunable dielectric properties.

5. Future aspect

The above discussion provides the possible applications of relaxor ferroelectrics in modern technologies. Besides the mentioned applications, the RFEs can also use in the field of multiferroics, pyroelectric, photoferroelectric, and so on. Hence, the requirement of relaxor ferroelectrics in the current ceramic market will increase significantly in the near future. Therefore, it is essential to focus on the research and development of RFEs in both academic and industry to find novel materials.

6. Conclusion

The present chapter describes the fundamental understanding of normal ferroelectrics to relaxor ferroelectrics and its possible applications in the modern technologies. The intriguing properties of relaxor ferroelectrics originate due to the presence of polar nano regions as a result of compositional fluctuation at the crystal structure. Although there are several theories available to explain the origin and dynamic of PNRs with external stimulus, it needs to establish the proper structure-properties relation for relaxor ferroelectrics. As per the material aspect, lead-based materials are dominating in the current markets. Therefore, the design of new lead-free relaxor ferroelectrics with enhanced physical properties is required for future applications.

Acknowledgements

Ths work was supported by Indian Institute of Technology Patna (IIT Patna).

Conflict of interest

The authors declare no conflict of interest.

Appendices and nomenclature

MPB	Morphotropic phase boundary
PNRs	Polar nanoregions
REFs	Relaxor ferroelectrics
MCW law	Modified Curie–Weiss law
BTO	$BaTiO_3$ (Barium Titanate)
BNT	$Bi_{0.5}Na_{0.5}TiO_3$ (Bismuth Sodium Titanate)
KNN	$K_{0.5}Na_{0.5}TiO_3$ (Potassium Sodium Niobate)
BKT	$Bi_{0.5}K_{0.5}TiO_3$ (Bismuth Potassium Titanate)
PZT	$PbZr_{0.48}Ti_{0.52}O_3$ (Lead Zirconate Titanate)

Author details

Lagen Kumar Pradhan and Manoranjan Kar*
Department of Physics, Indian Institution of Technology Patna, Patna, Bihar, India

*Address all correspondence to: mano@iitp.ac.in

Refrences

[1] Cross L E, Newnham R E, "History of ferroelectrics" American Ceramic Society (Ceramics and Civilizaion, Volume II: High-Technology Ceramics-Past, Present, and Future), 1987.

[2] Johnsson M and Lemmens P, Wiley Online Library, 2007. DOI: org/10.1002/9780470022184

[3] Ramesh R, Dutta B, Ravi T S, Lee J, Sands T, and Keramidas V G, Appl. Phys. Lett. 1994; 64: 1588

[4] Shkuratov S I, World Scientific, 2019, 456p. DOI:org/10.1142/10958.

[5] Mudinepalli V R, Leng F, Ceramics 2019; 2: 13-24.

[6] Nguyena M D, Nguyend C T Q, Vu H N, Rijnders G, Current Applied Physics 19; 2019: 1040-1045

[7] Jullian Ch, Li JF, Viehland D, J. Appl. Phys. 2005; 95(8): 4316-4318.

[8] Peláiz B A, García Z O, Calderón F, López N R, Fuentes B J, Phys. Sta. Sol. (b) (2005; 242(9):1864-1867

[9] Cross L E, Ferroelectrics 1987; 76: 241.

[10] Chang W A, *et al*., Journal of the Korean Physical Society 2016; 68: 12, 1481-1494.

[11] Pradhan L K, Pandey R, Kar M, J. Phys. Condensed matter 2020; 32: 045404.

[12] Alikin D, Turygin A, Kholkin A. Shur V, Ceramics Materials 2017; 10(1): 47.

[13] Smolienskii G A, J. Phys. Soc. Japan 1970; 28: 26-30.

[14] Viehland D, Jang S J, Cross L E, J. Appl. Phys. 1990; 68: 2916-2921.

[15] Quian H, Bursill L A, Int. J. Mod Phys. B 1996; 10: 2007-2025.

[16] Jin L, Li F, Zhang S J, J. Am. Ceram. Soc. 2014; 97: 1-27.

[17] Li F, Zhang S J, Damjanovic D, Chen L Q, Shrout T R, Adv. Funct. Mater. 2018; 28: 1801504.

[18] Wu J Y, Mahajan A, Riekehr L, Zhang H F, Yang B, Meng N, Zhang Z, Yan H X, Nano Energy 2018; 50: 723-732.

[19] Qu N, Du H, Hao X, J. Mater. Chem. C 2019; 7: 7993.

[20] Praharaj S, Rout D, Anwar S, Subramanian V, Journal of Alloys and Compounds 2017; 706: 502-510.

[21] Yoshida M, Mori S, Yazmamoto N, Uesu Y, Kiat J M, Ferroelectrics 1998; 217: 327-333.

[22] Caranoni C, Menguy N, Hilczer B, Glinchuk M, Stephanovich V, Ferroelectrics 2000; 240:241-248.

[23] Kumar A, Correa M, Ortega N, Kumari S, Katiyar R S, IntechOpen 2013. DOI: 10.5772/54298

[24] Rabe K M, Ahn C H, Triscone J M, Physics of Ferroelectrics: A Modern Perspective, springer 2007.

[25] Burns G, Dacol F H, Solid State Commun. 1983; 48: 853.

[26] Westphal V, Kleemann W, Glinchuk M, Phys. Rev. Lett. 1992; 68: 847.

[27] Vogel H, Physik Z. 1921; 22: 645.

[28] Fulcher G, J. Am. Ceram. Soc. 1925; 8: 339.

[29] Zheng S, Odendo E, Liu L, Shi D, Huang Y, Fan L, Chen J, Fang L,

Elouadi B, Journal of Applied Physics 2013; 113: 094102.

[30] Cross L E, ferroelectric 1994; 151: 305-320.

[31] Raddaoui Z, Kossi S E, Dhahri J, Abdelmoulab N, Taibi K, RSC Adv. 2019; 9: 2412.

[32] Macutkevic J, Banys, J. Bussmann H A, Bishop A R, Physical Review B 2011; 83: 184301

[33] Uchino K, Nomura S, Ferroelectr. Lett. 1982: 44: 55.

[34] Yu Z, Chen X, Physica B 2016; 503:7-10.

[35] Bokov A A, Ye Z G, Solid State Commun. 2000; 116: 105.

[36] Bokov A A, Bing, Y H, Chen W, Ye Z G, Bogatina S A, Raevski I P, Raevskaya S I, Sahkar E V, Phys. Rev. B 2003; 68: 052102,

[37] Shanming K, Huiqing F, Haitao H, H. Chan L W, Applied Physics Letters 2008; 93: 112906.

[38] Damjanovic D. Lead-Based Piezoelectric Materials: Piezoelectric and Acoustic Materials for Transducer Applications. Springer (Berlin); 2008. 59-79p. DOI: org/10.1007/978-0-387-76540-2_4

[39] Takenaka T, Nagata H, J. Eur. Ceram. Soc. 2005; 25: 2693-2700.

[40] Abdessalem M. B, Aydi S, Aydi A, Abdelmoula N, Sassi Z, Khemakhem H, Applied Physics A 2017; 123: 583.

[41] Aksel E, Jones J L, Sensors 2010; 10: 1935-1954.

[42] Kang M G, Jung W S, Kang C Y, Yoon S J, Actuators 2016; 5: 5.

[43] Liou Y C, Wu L, Huang J L, Yu C H, Japanese J. Appl. Phys. 2002; 41: 1, 3A.

[44] Duran, P, Lozano J F F, Capel F, Moure C, J. Mater. Sci. 1989; 24: 447-452.

[45] Kour P, Pradhan S K, Kumar P, Sinha S K, Kar M, Appl. Phys. A 2016; 122: 591.

[46] Augustinea P, Muralidhar M, Samantad S, Naik S P K, Sethupathid K, Murakamic M, Rao M S R, Ceramics International 2020; 46: 5658-5664.

[47] Wei H, *et al.* J. Mater. Chem. C 2018; 6: 12446.

[48] Shrout T R, Zhang S J, J. Electroceram 2007; 19: 113-126.

[49] Wang T, Jin L, Li C, Hu Q, Wei X, J. Am. Ceram. Soc. 2015; 98 [2]: 559-566.

[50] Seshadri R, Hill N A, Chem. Mater 2001; 13: 2892-2899.

[51] Reichmann K, Feteira A, Li M, Materials 2015; 8: 8467-8495.

[52] Veerapandiyan V, Benes F, Gindel T, Deluca M, A Review, Materials 2020; 13: 5742.

[53] Jan Abdullah, Liu H, Hao H, Yao Z, Cao M, Arbab S A, Tahir M, Appiah M, Ullah A, Emmanuel M, Ullah A, Manan A, J. Mater. Chem. C 2020; 8: 8962.

[54] Chauhan A, Patel S, Vaish R, Bowen C R, 2015; 8: 8009-8031.

[55] Valant M, Progress in Material Science 2012; 57: 980-1009.

[56] Kutnjak Z, Rozic B, Pirc R, Electrocaloric Effect: Theory, Measurements, and Applications .Wiley online library; 2015. 10.1002/047134608X.W8244

[57] Nguyen M D, Houwman E P, Rijnders G, J. Phys. Chem. C 2018; 122:15171-15179.

[58] Zhang L, Zhao C, Zheng T, Wu J, ACS Appl. Mater. Interfaces 2020; 12: 33934-33940

[59] Hanani Z, *et al.*, RSC Adv. 2020; 10: 30746.

[60] Yang C, Han Y, Feng C, Lin X, Huang S, Cheng, X, Cheng Z, ACS Appl. Mater. Interfaces 2020;12: 6082-6089.

[61] Singh A K, Pandey D, Yoon S, Baik S, Shin N, Appl. Phys. Lett. 2007; 91: 192904.

[62] Gao B, Yao Z, Lai, D, Guo Q, Pan W, Hao H, Cao M, Liu H, Journal of Alloys and Compounds 2020; 836:155474

[63] Dong G, Fan H, Liu, L, Ren P, Cheng Z, Zhang S, Current Science 2020; 118: 10

[64] Zhang Y, Liu H, Sun S, Deng S, Chen J, J Am Ceram Soc. 2021;104: 604-612.

[65] Rena, P, Liua Z, Liuc H, Sunc S, Wana Y, Longd C, Shie J, Chenc J, Zhao G, Journal of the European Ceramic Society 2019;39: 994-1001.

[66] Aman U, Kim W, Lee D S, Jeong S J, Ahn C W, J. Am. Ceram. Soc., 2014; 97 [8]: 2471-2478

[67] Zhang Ji, *et al*., Nature Communications 2015; 6:6615.

[68] Farnell G W, Cermak I A, Silvester P, Wong S K, IEEE Trans. on Sonics and Ultrasonics, 1970;17: 188.

[69] Maiti T, Guo R, Bhalla A S, Applied Physics Letters 2007; 90: 182901.

[70] Liu Z, Fan H, Zhao Y, Dong G, J. Am. Ceram. Soc. 2016; 99 [1]: 146-151.